# Design and operation of a high pulse rate intense ion beam diode

Cite as: Review of Scientific Instruments **66**, 3448 (1995); https://doi.org/10.1063/1.1145521
Submitted: 06 October 1994 . Accepted: 15 March 1995 . Published Online: 09 September 1998

W. A. Noonan, S. C. Glidden, J. B. Greenly, and D. A. Hammer

# Design and operation of a high pulse rate intense ion beam diode

W. A. Noonan,[a] S. C. Glidden, J. B. Greenly, and D. A. Hammer
*Laboratory of Plasma Studies, Cornell University, Ithaca, New York 14853*

(Received 6 October 1994; accepted for publication 15 March 1995)

Virtually all practical applications for intense ion beams require that the beam pulses be generated at high repetition rates. This paper reports the development of the first high pulse rate, long-lived ion beam diode. It is a magnetically insulated diode which has produced ~75 keV proton and carbon beam pulses of 1.0–2.5 A/cm$^2$ and 100 ns duration at up to 90 Hz in four pulse bursts. It has also produced 125 keV, 5 A/cm$^2$ Ar beams at a steady 1 pulse per 30 s for over 1000 pulses between failures in many runs. This diode employs a magnetically confined anode plasma ion source, and the high repetition rate pulsed power systems are based upon saturable magnetic switching. © *1995 American Institute of Physics.*

## I. INTRODUCTION

Research on intense ion beams and on the ion diodes which produce these beams has been motivated for about two decades principally by potential applications in both inertial and magnetic confinement fusion.[1–7] Such beams are also attractive for processing of special purpose materials,[8,9] including annealing semiconductors,[10] modifying the surface properties of metals,[11] ion implantation,[12] and thin film production.[9] All of these potential applications for intense ion beams require that they be pulsed at rates in excess of about 1 Hz and have long component lifetime. For instance, the LIBRA design study[13] for a light ion beam driven inertial confinement fusion reactor calls for 3 Hz pulse rates, which would accumulate over 20 000 pulses per day. Further, having a high average pulse rate would also provide a unique opportunity for investigating ion diode and beam physics by making possible the collection of many data points.

Prior to the work reported here, all ion diodes in our laboratory had been limited to a few tens of pulses per hour at best, with a time between failures of at most a few tens of pulses. If any of the potential applications noted above are ever to be realized, the question of how to build an ion diode capable of pulsing at a high repetition rate must be addressed. In this paper we describe a first attempt at this, namely a system called RRAIDER (rep-rate ion diode experiment) that has produced 75 keV mixed proton and carbon beams with 1.0–2.5 A/cm$^2$ and 100 ns duration at up to 90 Hz in four pulse bursts. The burst length was limited by magnetic field coil heating, and the repetition rate was limited by failure of the Faraday Cup ion beam monitor. The device has also produced 125 keV, 5 A/cm$^2$ argon beams at a steady 1 pulse per 30 s for over 1000 pulses between failures in many runs with essentially no degradation of performance within a run. This system employs a magnetically insulated diode (MID) with a magnetically confined anode plasma ion source, and its high repetition rate pulsed power systems are mostly based upon saturable magnetic switching.

[a]Current address: Plasma Physics Division, Naval Research Laboratory, Washington, DC 20375-5346.

## II. DIODE DESIGN

### A. General considerations

The problems with building a high pulse rate ion diode fall into two broad categories: recovery time between pulses, and minimizing (or eliminating) routine component damage per pulse.[14] In most commonly used ion diodes,[15] plasma and large amounts of neutral gas are left behind after each beam pulse and must be removed before the diode can be operated again. Additionally, in the case of the magnetically insulated diode which is used in the present work, ion and electron bombardment of the diode's internal structures and resistive losses in the diode's magnetic field coils produce a heat load which must also be removed.

Component damage to the ion diode can occur in many forms. For example, ion and electron bombardment can cause erosion and spallation of structures and electrons also induce insulator breakdown. The diode structures can also exhibit mechanical fatigue and embrittlement from the large electromagnetic stresses that they experience. Finally, the erosion is very rapid on the most common ion source for magnetically insulated diodes, the surface flashover source; rarely does one last more than 100 pulses.

At the outset of this work, the goal was to build and demonstrate the first high pulse rate, long-lived ion diode. The biggest obstacles to high pulse rate operation of standard MIDs were gas loading and wear on the ion source. Consequently, these were the problems on which this work focused. The need for cooling was circumvented by operating the diode either for short bursts of pulses at the high pulse rates or at the relatively low rate of 2 pulses per min in continuous operation. At the relatively low beam power (2 GW peak) and ion current density of a few A/cm$^2$ for 100 ns in our experiment, called RRAIDER, ion bombardment damage was not a problem. Furthermore, the final design reported on in this paper did not have a significant problem with electron damage. Although the pulsed power system hardware from the decommissioned ETA accelerator[16] on which RRAIDER was based was capable of 1 kHz operation, residual gas removal was expected to limit ion diode repetition rate to at most a few hundred Hz. As will be described shortly, we achieved a 90 Hz pulse rate in practice.

First consider the problems of electron and ion induced

 0034-6748/95/66(6)/3448/11/$6.00 

erosion of diode components. Electron induced damage is minimized by designing the magnetic field configuration of the magnetically insulated diode to reduce electron losses as much as possible. Ion bombardment of surfaces can be minimized by simply not putting anything in the path of the ion beam, i.e., by not using a material cathode. Many MIDs already employ such a "virtual" cathode,[15] in which electrons emitted from metal cathodes on the periphery of the diode can flow along the magnetic field lines to form a virtual electrode in front of the anode.

The principal origin of the gas loading, which limits diode recovery between pulses, is the ion source. Surface flashover sources typically eject $10^2$–$10^5$ times more neutrals than ions,[17] which helps explain its limited life. If the anode plasma is generated by efficiently ionizing a localized puff of gas and magnetically confining the resulting plasma at the desired anode position, then it is possible to eliminate the gas loading and anode wear problems at the same time. This was the goal of the magnetically confined anode plasma (MAP) ion source, which was originally fielded on a pulser called LONGSHOT.[18,19] In that experiment, 1-$\mu$s-long high purity beam pulses of 75–150 keV protons were produced at current densities exceeding 100 A/cm$^2$ at up to a few pulses per hour[19] (limited by the pulsed power drivers).

The diagram for our cylindrically symmetric extractor diode, employing a MAP diode and an inductive acceleration structure, is shown in Fig. 1. The anode plasma in an ion diode such as this is created by a sequence of steps. First, a "slow" magnetic field is applied on a 100 $\mu$s time scale which has a minimum-$B$ configuration well back from the anode–cathode gap. Then a localized puff of gas is introduced into the region of the field null, where it is more easily ionized and where the resulting plasma is partially confined. Third, the gas is "preionized" to initiate plasma formation. Finally, a fast ($\lesssim$1 $\mu$s) rising magnetic field is superimposed on the already existing "slow field." By virtue of its large $\partial\mathbf{B}/\partial t$, the "fast field" induces a large azimuthal electric field in the preionized gas puff (about 350 V/cm in the center of the puff) which causes avalanche breakdown. Furthermore, as the fast field increases, it modifies the total magnetic field such that the flux surfaces upon which the anode plasma resides are pushed toward the cathode. Since the plasma electrons are highly magnetized, the electrons move with the flux surfaces, and the resulting space charge electric field pulls the ions along. This motion also serves to separate the plasma from the remaining neutrals in the gas puff.

In the general vicinity of the acceleration gap, the magnetic field strength increases along the flux lines as they are followed radially away from the gap, as we will describe shortly. Therefore, the anode plasma is mirror-confined radially. When the plasma reaches the desired position in the axial direction, the main voltage pulse is applied in order to extract an energetic ion beam. The distance between the anode plasma and the virtual cathode electron cloud defines the acceleration gap spacing.

In a MAP ion source, the gas puff is a radially expanding gas cloud near the rear surface of the diode. During the period between pulses, this gas cloud and the recombined anode plasma expand to fill the entire diode and constitute most

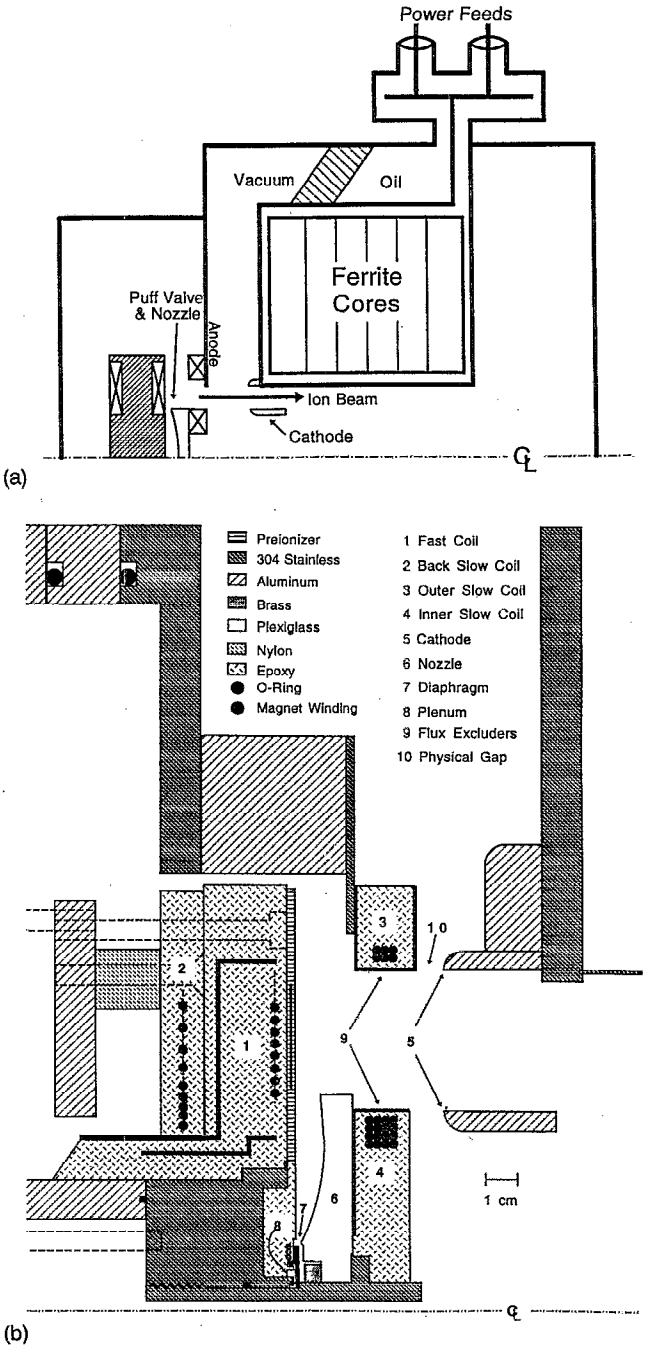


FIG. 1. The design of RRAIDER: (a) schematic layout, and (b) mechanical drawing of the diode.

of the gas load that must be pumped out between pulses. The largest possible gas loading that RRAIDER's MAP source could impose on its vacuum system occurs if the puff valve empties the entire contents of its plenum. In RRAIDER, the plenum volume is 0.28 cm$^3$ and it is filled to 0.02–1 atm, depending upon the gas. This implies a maximum gas load of about $10^{19}$ molecules at most. By contrast, a flashover source fielded on LONGSHOT ejected an estimated $10^{21}$ neutrals into its vacuum chamber.[17] In practice, the left over puff gas is easily pumped out in a few milliseconds.

The MAP source has several other advantages which are important for both single pulse and high pulse rate operation. For one, the MAP source can produce pure ion beams of

many different species by merely changing the puff gas; nitrogen, proton, and argon beams have already been produced. The MAP source also has the advantage over passive sources that the ions are present before the main voltage pulse. Therefore, there is not any turn-on delay during which no ion beam is being generated due to the time required to form an anode plasma ion source. However, there can still be a turn-on delay due to the formation of the virtual cathode after the application of the acceleration voltage to the gap.[20]

## B. RRAIDER subsystem design and operation

### 1. The gas puff source

The gas puff source[21] consists of a puff valve and a nozzle [items 6–8 in Fig. 1(b)] which create a radially expanding layer of gas in front of the fast field coil (item 1). The intent is to produce ~100 mTorr gas pressure in the layer without spoiling the vacuum in the acceleration gap. The puff valve uses a 4.3-cm-diam annular diaphragm (item 7) made from a high conductivity, heat treated beryllium–copper alloy which is stamped into a conical shape to form a Belleville (constant force) spring.[22] The diaphragm seals against two O rings and covers an annular gas plenum (item 8). Pulsing 10 kA current through a coil behind the diaphragm generates a magnetic force on the diaphragm approximately 10 times its spring force and pushes the valve open. The diaphragm thickness is minimized to reduce its mass, but it is thick enough to act as a flux excluder on the time scale of the driving pulse and also to ensure sufficient mechanical strength. In order to achieve the necessary sharp density gradient at the front of the gas puff, the diaphragm must be pushed away from the O rings in a time less than or comparable to the time it takes the gas to move a few cm. For hydrogen at room temperature, this requires a few tens of microseconds or less, and so a 17 $\mu$s half-period electrical pulse powers the puff valve coil. Operating the puff value at 10 kA results in a terminal diaphragm velocity greater than $10^3$ cm/s, while 6.5 kA yields about $4.5\times10^2$ cm/s. The lower current value is adequate to obtain the necessary gas puff pressure in the plasma formation volume in front of the fast coil. Valve opening takes less than 50 $\mu$s with this current.

Ideally, the puff valve should reclose quickly to minimize the vacuum recovery time. After opening, the diaphragm bounces off the acrylic nozzle structure [item 6 in Fig. 1(b)] and closes as rapidly as it opens. When it returns to its original location, most of its energy is absorbed by an inelastic collision with the O-ring seal. As a result there is very little opening on the second bounce.

Operated at 6.5 kA, the puff valve in its final version operated for many thousands of pulses without failure.

The gas source was characterized by series of measurements performed with a fast ionization gauge (FIG). After Pedrow,[23] we used a 6AU6A pentode tube as the gauge. We designed and built a controller to be used with this tube that actively stabilized the emission current. This system has a 10 $\mu$s response time and is dc calibrated against a Granville–Phillips series 275 Convectron gauge. Typical pressure pulses for argon gas are shown in Fig. 2. The pulse-to-pulse

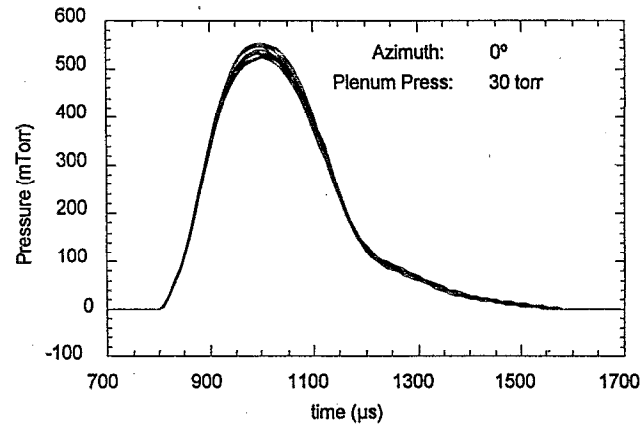


FIG. 2. Typical pressure pulses from the puff valve measured at a radius of 9 cm, for argon at a 30 Torr plenum pressure. The pulse-to-pulse variation is ±5%.

reproducibility in amplitude is ±5%. We found that the gas layer has a very sharp boundary; the 10%–90% width is at most 5 mm (Fig. 3). Unfortunately we could not measure the actual thickness of the gas layer because of the size (~1 cm) and shape of the pentode tube. The peak pressure in the gas layer can be varied by either changing the pressure in the puff valve's plenum or by changing how hard the diaphragm is driven (Fig. 4). The azimuthal uniformity of the gas cloud is rather good (Fig. 5). Originally there was higher pressure at the position where a gas feed tube fed the plenum. We solved this problem by placing a flow limiter in the feed tube.

In practice we varied the plenum pressure and, hence, the puff pressure to accommodate the different breakdown characteristics of the three gases we used in experiments, hydrogen, argon, and acetylene. Hydrogen, which is difficult to break down, required a 900 Torr plenum pressure, while argon and acetylene worked best with plenum pressures in the range of 20–100 Torr.

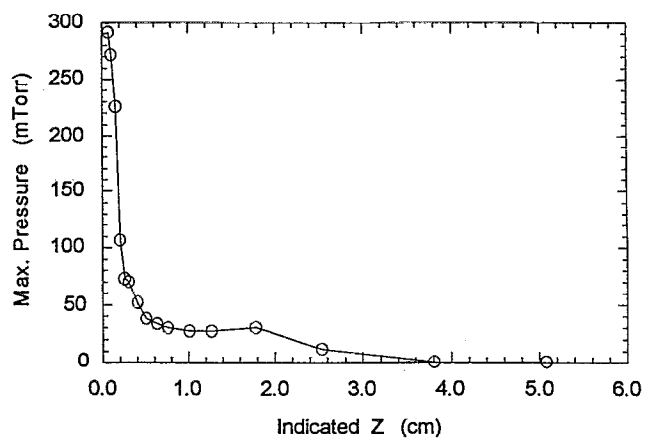


FIG. 3. Variation of puff gas layer pressure with position of the fast ionization gauge (FIG) at a radius of 9 cm, for argon at a 30 Torr plenum pressure. (At $z=0$ in this graph, the FIG is actually centered in the nozzle opening. Increasing $z$ means farther away from the fast coil surface.)

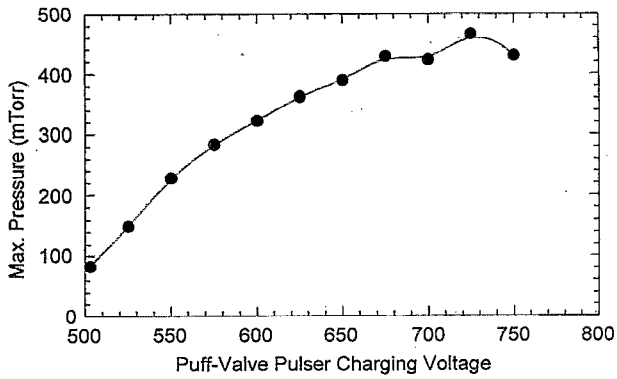


FIG. 4. The puff pressure can be increased by driving the diaphragm harder, which is accomplished by increasing the amplitude of the current pulse (which scales with the puff-valve driver charging voltage) that drives the puff valve's magnetic field coil. These data are for argon at a 30 Torr plenum pressure.

## 2. The preionizer

While the gas puff is ionized mostly by the electric field induced by the rising "fast" magnetic field, we found empirically that preionization is essential to achieving reproducible results. This probably happens because avalanche breakdown depends critically on the initial supply of free electrons.

We initially used an array of surface flashover gaps located around the outer circumference of the fast coil which were intended to produce intense UV radiation for preionization. In fact, the UV illumination was not intense enough and preionization was mostly a result of plasma injected from the flashover gaps. This was deduced from the length of the time delay between pulsing the preionizer and pulsing the fast coil that was needed for optimal performance. This inference is also supported by the fact that the preionizer had to be located within the low magnetic field region near the fast coil to have any effect. Surface flashover plasma preionization is undesirable because it mixes impurities into the ion beam. Further, the gap-to-gap and shot-to-shot variations in the flashover source output result in poor uniformity and poor reproducibility of the final anode plasma.

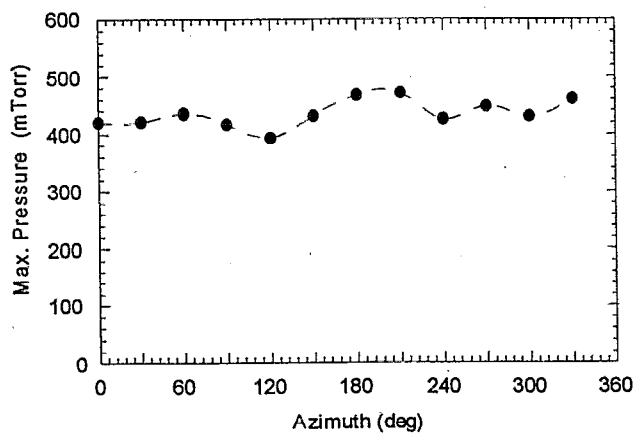


FIG. 5. Azimuthal uniformity of the gas puff, for argon at a 30 Torr plenum pressure. Each data point is from a single and separate pressure pulse.

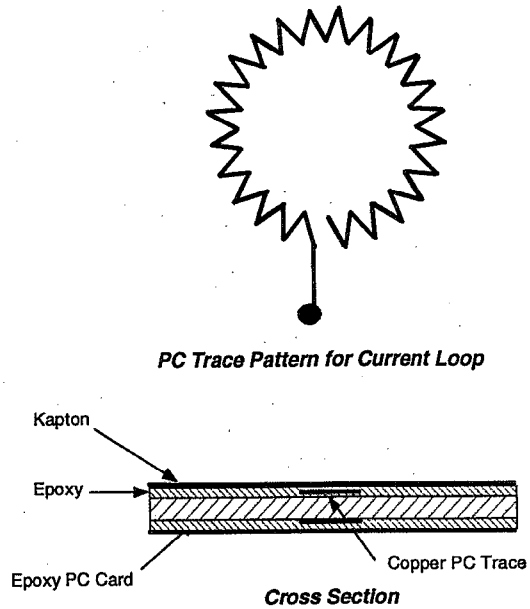


FIG. 6. Inductive preionizer construction.

The final RRAIDER design uses an inductive preionizer. A radially localized and approximately azimuthally symmetric region of rapidly time-varying magnetic fields produce the initial electrons for the avalanche breakdown of the gas. The preionizer is made by etching a pattern of conductors on the surface of a copper clad G-10 epoxy circuit board and bonding a sheet of 0.002-in.-thick Kapton over it with a thin layer of epoxy. This board is then attached to the front surface of the fast coil. The inductive electric fields are strongest immediately over the printed circuit traces, and that is where the puff gas preferentially breaks down. Consequently, the best preionizer is the one that maximizes the PC trace area. Several different patterns have been tried, and the star pattern shown in Fig. 6 provided the best results. The return current path is circular at the mean radius of the star and on the backside of the circuit board. This minimizes the inductance of the preionizer so as to maximize the peak current and frequency of the driving pulse. It also reduces the coupling to the fast coil circuit. This preionizer provides a high level of pulse-to-pulse reproducibility.

## 3. The field coils

As described earlier, there are two magnetic field components in a MAP diode. The quasistatic "slow field" is generated by three coils [items 2, 3, and 4 in Fig. 1(b)] which are energized by a 70 $\mu$s half-cycle current pulse. A plot of the slow field's flux surfaces is shown in Fig. 7(a). The fast field coil is located just in front of the back slow field coil and acts to boost its effect. Plots of the flux surfaces for the total field as the fast field gains strength are shown in Figs. 7(b) and 7(c). Note how the flux surfaces for the total field are gradually pushed forward. These flux surfaces were calculated using the MSUPER code and were verified by B-dot loop measurements. For the experiments described here, the strength of the magnetic field is a few kilogauss at midgap

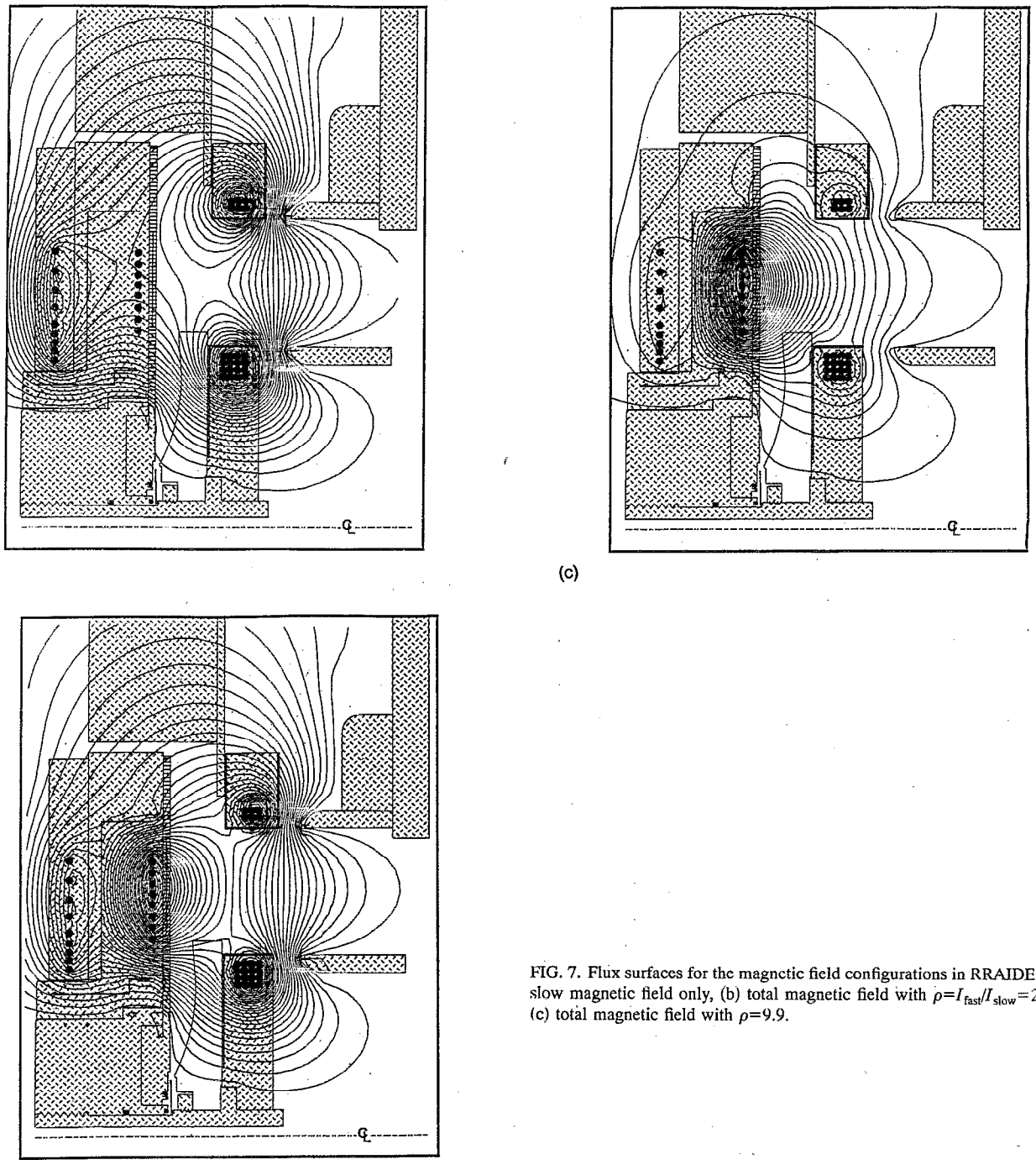


FIG. 7. Flux surfaces for the magnetic field configurations in RRAIDER: (a) slow magnetic field only, (b) total magnetic field with $\rho=I_{fast}/I_{slow}=2$, and (c) total magnetic field with $\rho=9.9$.

and at a 9 cm radius. The strength of the slow and fast magnetic fields are independently adjustable in the experiment.

The slow field coils are shielded by flux excluders in order to protect them from the large voltages induced by the fast field coil. For the inner and outer slow coils, the shields are 15-mil thick stainless steel cases. The thickness was carefully chosen such that they are flux excluding on the time scale of the fast field but not on the time scale of the slow field, thereby allowing the slow field to penetrate into the gap. These flux excluders are an intrinsic part of the magnetic field design and are included in the MSUPER calculations. Indeed, the careful placement of flux-excluding structures is very important to the successful operation of the diode. For instance, we found that the cathode tips must be placed outside of the inside edges of the inner and outer slow coil flux excluders. Otherwise too much curvature is introduced into flux surfaces between the cathode tips and the flux excluders. The electrons then leak across the acceleration gap via curvature drift, electron damage increases, and the diode efficiency drops.

### 4. The acceleration gap

The acceleration gap is determined by the positions of the virtual cathode electron cloud and the anode plasma

TABLE I. Diode specifications.

| | |
|---|---|
| Outer beam radius | 10.8 cm |
| Inner beam radius | 6.5 cm |
| Accelerating voltage | 120 kV @40 kA and 100 ns FWHM |
| Physical gap | 8 mm |
| Insulating field | 4 kG @ mid-gap and radius=9 cm |

when the acceleration voltage is applied. These two plasmas make electrical contact with the metal cathode tips and the slow coil flux excluders, respectively, and it is across the "physical gap" made by these mechanical structures that the acceleration voltage is applied. This physical gap is part of an inductive accelerating structure since it is the secondary circuit of a one-turn ferrite core transformer [Fig. 1(a)].[16] This was highly advantageous because our diode has four independent pulsed power subsystems (for the puff valve, preionizer, slow coil, and fast coil), all of which must be at anode potential. On the other hand, all of the beam diagnostics must be at cathode potential. With an electrostatic accelerator, either the four pulsed power systems or the diagnostics must float at 100 kV. In contrast, inductive acceleration allows us to keep everything at ground potential.

The inner bore of the ferrite core transformer determined the outer radius of the diode. In turn, this constraint and the volt-second product of the ferrite core dictated all of the other diode specifications, which are summarized in Table I.

### 5. Overall system operation and plasma production

The five independent pulsed power subsystems of RRAIDER were capable of pulse repetition rates up to 1 kHz, determined largely by the decommissioned ETA hardware we utilized.[16] The puff valve and preionizer subsystems were powered by high power silicon-controlled rectifier (SCR)-switched capacitor banks followed by several stages of magnetically switched pulse compression, and the main acceleration voltage was provided by a thyrotron-switched capacitor bank followed by three stages of magnetically switched pulse compression.[24] The fast coil power pulse was compressed by a gas-switched capacitor circuit because a ferrite core with the required volt-second product needed for magnetic switching was not available. Finally, the slow coil was powered directly by a SCR-switched capacitor bank without pulse compression. Pulsed power system details may be found elsewhere.[21,24] Each of the five subsystems is pulsed as depicted in Fig. 8 to produce the diode operation described at the beginning of this section.

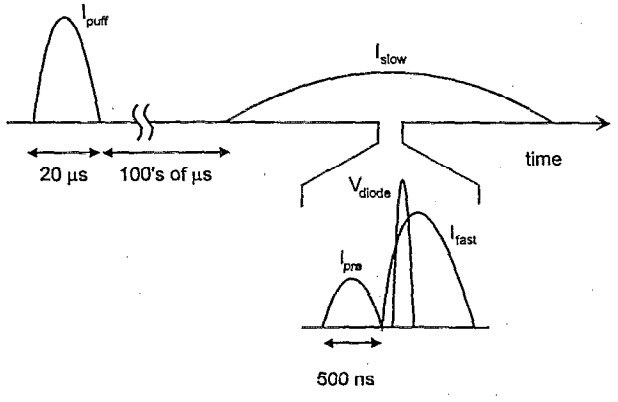


FIG. 8. Schematic illustration of the pulsing sequence for RRAIDER. $I_{pre}$, $I_{slow}$, etc., are the current pulses driving the inductive preionizer, slow coil, fast coil, and preionizer. $V_{diode}$ is the main accelerating voltage pulse.

The density and temperature of the anode plasma produced when hydrogen gas was used was determined with Langmuir probes and by plasma spectroscopy.[25] The result was $n_e \sim 10^{14}/\text{cm}^3$ and $T_e = 2$–$3$ eV. Therefore, in the >0.1 T magnetic fields in and near the diode accelerating gap, the plasma is low beta (ratio of particle pressure to magnetic pressure) and the electrons are strongly magnetized. Similar measurements were not made using argon or acetylene, but we have no reason to believe that plasma conditions were substantially different in those gases.

## III. DIODE PERFORMANCE

Many different gas species have been used to make beams with this diode, including hydrogen, nitrogen, argon, and acetylene. However, most of the work reported here deals with argon beams or with mixed carbon and proton beams extracted from acetylene. Acetylene was a convenient gas from which to make anode plasmas because its low Paschen minimum made it easy to ionize. Argon has a similar advantage, although not to the same extent. However unlike acetylene, experiments with an argon puff gas produced single species beams of $Ar^+$. We saw no spectroscopic evidence of $Ar^{++}$.

RRAIDER has been operated both at rates up to 90 Hz in bursts of up to four pulses and in a "single pulse" mode at 1 pulse per 30 s for over 1000 pulses between failures. Burst mode operation permitted a determination of the diode recovery time. Single pulse operation in long runs enabled us to evaluate life-limiting components and determine reproducibility.

### A. Single pulse operation

Typical diode voltage, current, and impedance histories for hydrogen beam production are shown in Fig. 9. The diode current, measured with Rogowskii coils, is the total current flowing through the diode: the ion beam current plus the electron leakage current due to imperfect magnetic insulation. The diode voltage is the electric potential across the physical acceleration gap and is deduced from the voltage drop measured at the power feed to the ferrite core transformer [see Fig. 1(a)]. The power feed and diode voltages differ by an inductive voltage caused by a time-varying current, $dI/dt$, flowing around the vacuum chamber walls and through diode mounting supports to the inner and outer slow coil flux excluding jackets which form the anode side of the gap. Diode voltage $V_d$ is, therefore, determined by measuring the self-inductance, $L$, of this current path, and subtracting $L dI/dt$ from the power feed voltage. We measured $L$ by shorting out the accelerating gap so that the voltage drop measured at the power feed was entirely inductive. The inductance is then easily calculated from simultaneous measurements of the power feed voltage and the diode current, $I_d$.

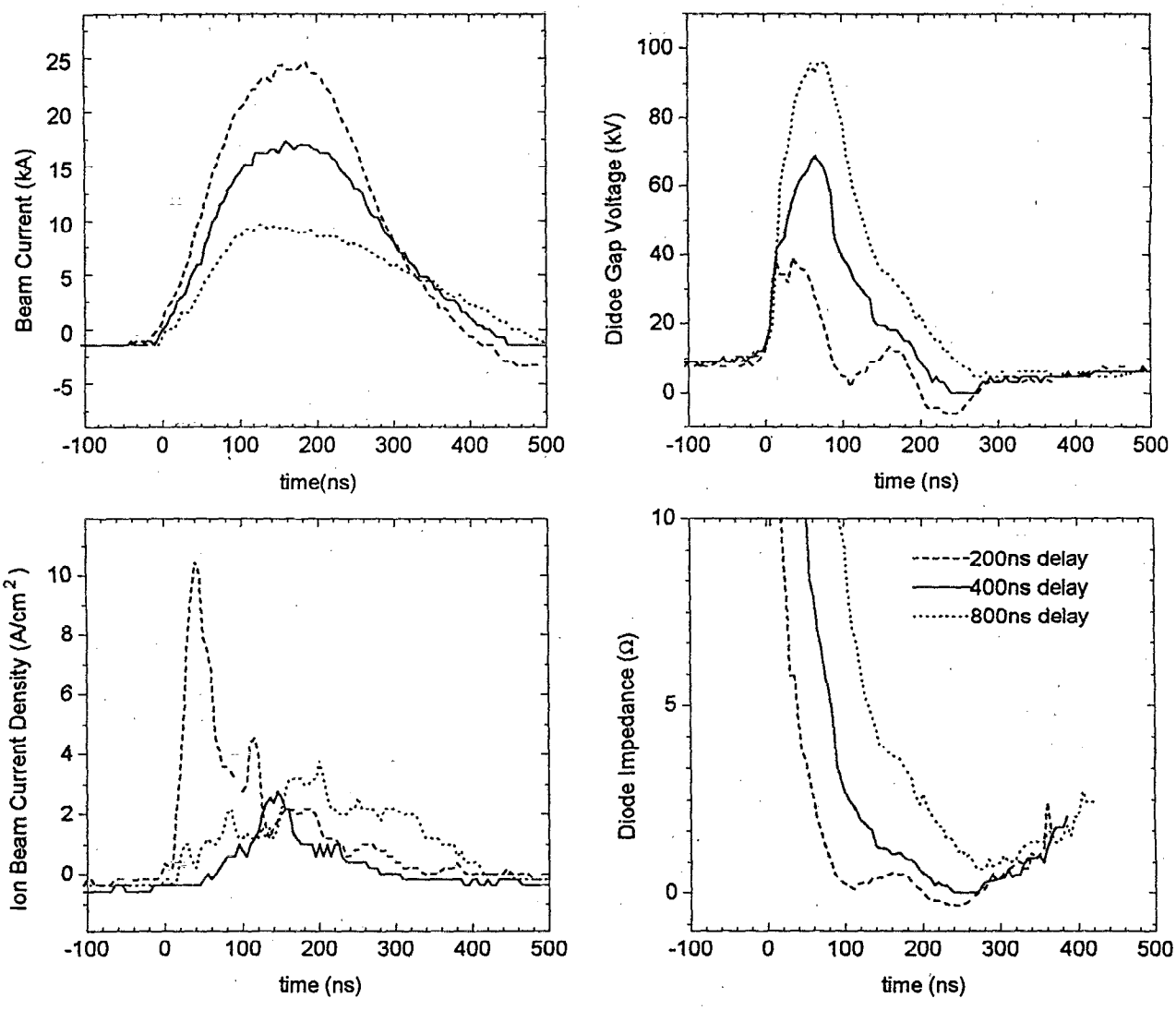


FIG. 9. Diode voltage, beam current, and impedance histories for high, low, and intermediate impedance operating conditions. Beam current densities measured with a Faraday cup are also shown. The different operating conditions were obtained by changing the delay of the accelerating voltage pulse relative to the rising edge of the fast field. Relative delays of 200, 400, and 800 ns gave impedances 13.7, 5.3, and 0.8 Ω at peak power. Hydrogen at a 900 Torr plenum pressure was used for these beam pulses.

Traditional magnetically insulated diodes with passive ion sources have impedances that typically fall with time. MAP diodes, on the other hand, can be adjusted to produce falling, rising, or steady impedance histories.[19] We obtained different impedance histories by varying the location of the magnetic flux surface at the front of the anode plasma relative to the accelerating gap. In practice this is acccomplished by delaying the main voltage pulse with respect to the rising edge of the current pulse which drives the fast field coil. Figure 9 shows the diode voltage, impedance, and beam current histories for three relative delays with hydrogen gas puffs. Figure 10 shows the diode impedance at the time of peak power ($=V_d \times I_d$) as a function of main voltage pulse delay using acetylene gas puffs.

We made detailed measurements of ion beam current densities for $Ar^+$ beams and typically found about 2 A/cm$^2$. The diode voltage was typically about 100 kV, and so the Child–Langmuir ion current density $j_{CL}$ for the nominal 1 cm physical gap in our diode was 200–300 mA/cm$^2$. This

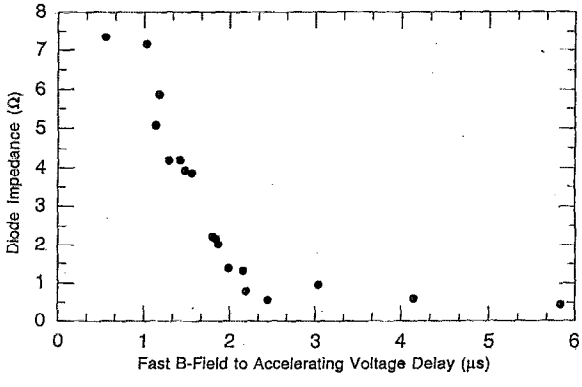


FIG. 10. Impedance variation of RRAIDER's MAP diode is a function of the delay between initiating the fast coil current and the acceleration-gap voltage pulse. The impedance shown is at the moment of peak diode power during the acceleration gap voltage pulse. These data are from acetylene pulses with a 100 mTorr plenum pressure.

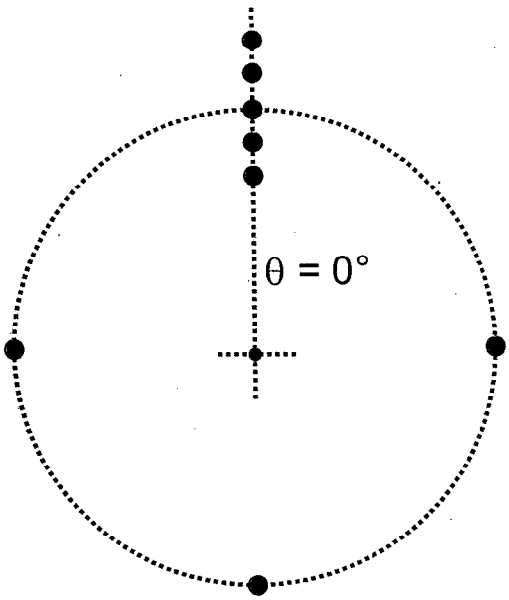


FIG. 11. Positions of the Faraday cups in their array.

means that the diode was performing with a current enhancement of a factor of 5–10 at peak current density, which is typical of MIDs. The active anode area is about 300 $cm^2$, which implies that the total beam current was approximately 600 A. Since the total diode current was about 15 kA, the diode operated with only 4% efficiency. In contrast, MIDs routinely produce proton beams with efficiencies exceeding 50%. Much of this difference can be attributed to the fact that $j_{CL} \sim 1/\sqrt{m_i}$, where $m_i$ is the ion mass, implying 6.3 times lower efficiency due to argon's greater mass.

We used Faraday cups arrayed at positions shown in Fig. 11 to map out the argon ion beam current density as a function of radius, azimuth, slow magnetic field intensity, and fast magnetic field intensity (Fig. 12). The magnetic field intensities are characterized by two parameters. The first is the ratio between the currents in the fast and slow coils, $\rho \equiv I_{fast}/I_{slow} \propto |\mathbf{B}_{fast}(x)|/|\mathbf{B}_{slow}(x)|$. (Note that $\rho$ is independent of position even though the magnetic fields are not.) This parameter is a measure of how far out into the gap the flux surfaces carrying the anode plasma are pushed. The second parameter is simply the current in the fast field coil. Since both $\mathbf{B}_{slow}$ and $\mathbf{B}_{fast}$ scale with $I_{fast}$ for constant $\rho$, the fast coil current is a measure of the total magnetic insulation of the gap. Each data point in Fig. 12 is an average of five pulses. As can be seen, the beam current density depends strongly on both the shape and the overall strength of the insulating magnetic field. Further, different field configurations yield optimal ion beam current densities at different positions in the beam annulus.

## B. Pulse-to-pulse reproducibility in single pulse operation

Although good reproducibility of the diode's operation depends on many factors, it rests fundamentally on the pulse-to-pulse reproducibility of the pulsed power systems. Not only must the pulse magnitudes be consistent, but also the timing jitter needs to be small. The variations of pulsed power and iodide parameters are presented in Table II. Although the diode voltage, current, and impedance histories are reproducible, there is still a lot of scatter in the beam current density. The distributions of the data are decidedly non-normal. Therefore, their statistical spread is calculated in nonparametric (distribution-free) terms. What is reported in Table II is the ratio between the population medians and interquartile distances:

$$\delta = \frac{\xi_{0.75} - \xi_{0.25}}{\xi_{0.5}}, \tag{1}$$

where $\xi_q$ is the $q$th population quantile.

TABLE II. Diode and pulsed power pulse-to-pulse variation.

| Parameter | $\delta$ |
|---|---|
| Peak slow coil current | <1/2% |
| Peak fast coil current | 1/2% |
| Fast coil current at time of accelerating voltage pulse | 1% |
| Puff pressure | 5% |
| Diode voltage[a] | <5% |
| Diode current[a] | 5% |
| Diode impedance[a] | 10% |
| Beam current density[a] | 30% |

[a]These are typical values. The specific value depends upon the magnitudes chosen for the fast and slow magnetic fields.

The jitter in the relative delay between the acceleration voltage pulse and the fast coil current pulse is particularly important, because it determines the strength of the fast field at the time of beam formation. This jitter was ±7 ns, which was apparently adequate for reproducible diode operation.

## C. High pulse rate operation

RRAIDER was operated in burst mode at pulse rates from 1 up to 90 Hz, where we began to see a significant decline in ion beam current density as measured by the Faraday cups during the course of a burst. Diode current, diode voltage, and Faraday cup signals for a four pulse burst at the maximum pulse rate of 90 Hz are shown in Fig. 13. In this case, 35–50 keV beams were produced from acetylene puffs. The Faraday cup was placed at a 9 cm radius and 5 cm downstream from the acceleration gap in a magnetic field free region. At this pulse rate, there is a significant pulse-to-pulse spread in diode impedances and diode voltages. This, no doubt, created significantly different virtual cathodes and beam extraction. Nevertheless, beams were produced on each pulse.

At the 90 Hz repetition rate, after a couple of strong pulses, the Faraday cup signal always dwindled away during a burst. This effect was made less pronounced by either decreasing the pulse rate or by increasing the area of the cup's aperture. This fact, together with the fact that the Faraday cup signal amplitude was not correlated with fluctuations in the acceleration voltage suggest that this problem is connected with the Faraday cup's operation rather than a limitation in the diode's performance. Further, the fact that lowering the pulse rate also improved the cup's performance

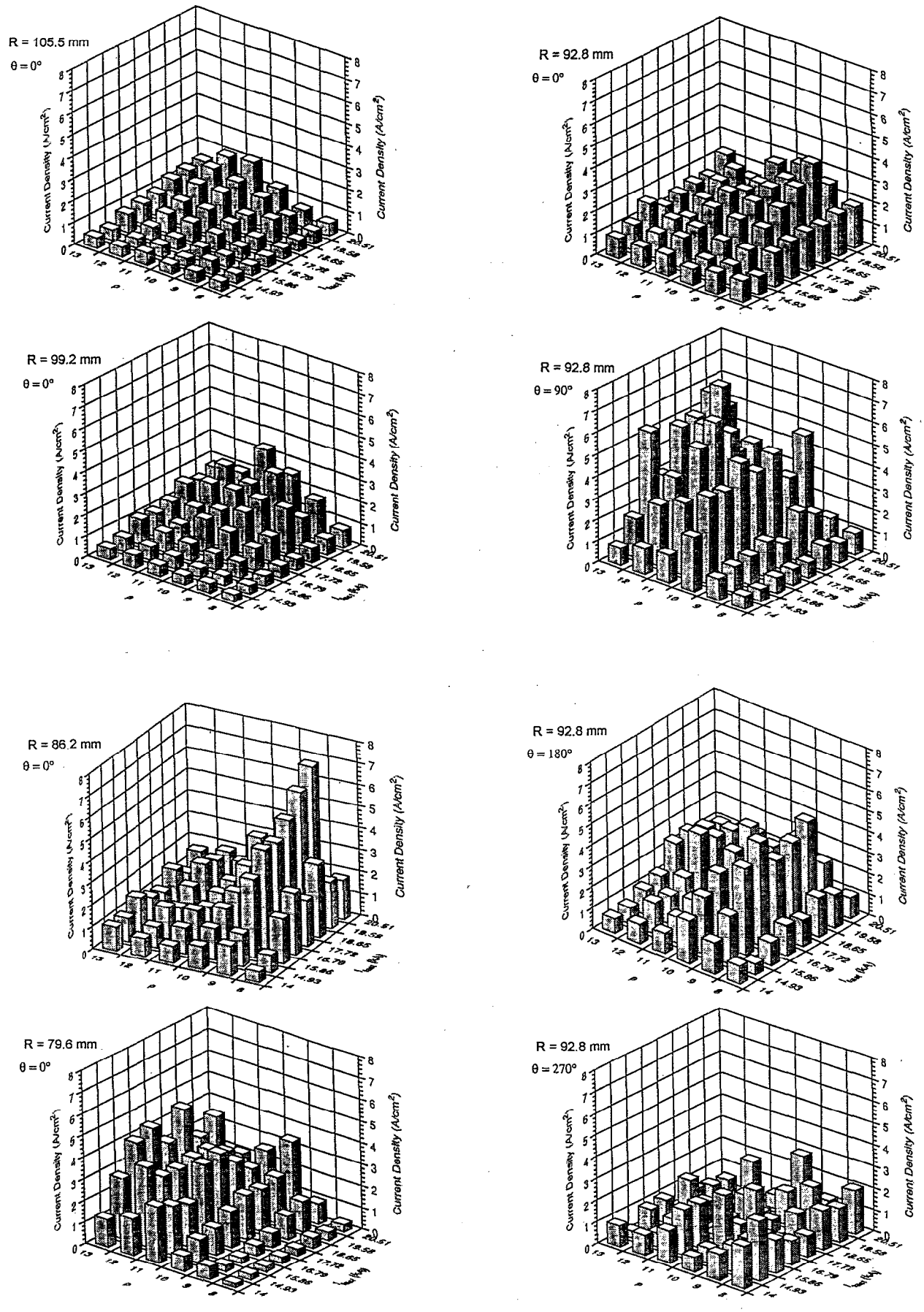


FIG. 12. Ion beam current density vs radius, azimuth, $\rho$ and $I_{fast}$.

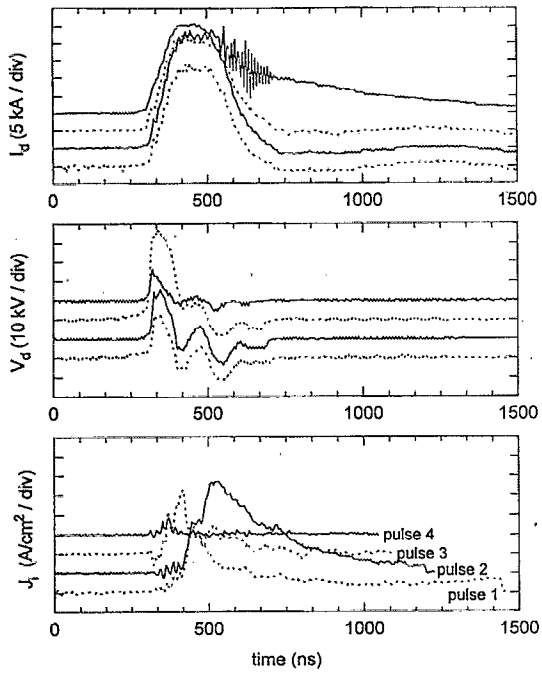


FIG. 13. Typical (a) diode current, $I_d$, (b) diode voltage, $V_d$, and (c) ion beam current density, $J_i$, data for a 90 Hz four pulse burst. Successive traces are displaced vertically upward for clarity.

suggests that the problem is with the recovery of the cup between beam pulses. The recharging time for the Faraday cup's bias capacitors is shorter than the delay between beam pulses. Moreover, plasma generated at the Faraday cup has plenty of time to recombine, and neutral gas generated by the desorption of gases and/or sputtering of metal atoms from the cup's outer surfaces by the ion beam has plenty of time to move away from the cup at thermal velocities in 10 ms. This leaves the possibility that neutral gas generated inside the cup caused the Faraday cup signals to gradually decrease at the higher repetition rates, since decreasing the cup aperture did exacerbate the problem. In the burst shown in Fig. 13, the second pulse exhibits a large and abnormally long Faraday cup signal, suggesting a gas discharge within the cup. Perhaps sufficient energy is deposited by the complete discharge of the bias capacitor to fill the cup with more neutrals than can be pumped out in 10 ms.

The cause of the pulse-to-pulse voltage fluctuations within a burst at high pulse rate, which is evident in Fig. 13, is not known at this time.

### D. Discussion

In the course of achieving burst mode operation at up to 90 Hz and also long runs at 1 pulse per 30 s, we improved the component reliability and longevity which is needed for high average pulse rate devices. RRAIDER can typically be pulsed over 1000 times before having to make minor repairs or replacements. In experiments carried out to study ion diode physics,[20] many $\gtrsim$1000 pulse runs were taken without a major component failure. The most common failure involved the preionizer circuit board, suggesting the need for developing improved construction methods for that component.

In the past, experimental investigations have been hampered by relatively low pulse rates which have allowed the collection of only rather sparse data sets. Furthermore, the pulse-to-pulse reproducibility has been poor due to the uncontrolled nature of some of the diode processes, like the flashover mechanism in flashover anodes. The advent of this high pulse rate diode has rectified this situation to some degree. In addition, the collection of many data points puts diode experiments on a statistical basis for the first time. This development is important in light of the pulse-to-pulse variations exhibited by ion diodes. It allows one to assemble a clearer and more complete picture of diode behavior and avoids the dangers of making inferences from a small, variable data set. In particular, these capabilities have been used to make the first direct measurement of the electron density distribution in the diode gap.[20]

The next major step in achieving a true high average power ion diode, the design, construction and testing of an actively cooled MAP diode, is now in progress.[26] The goal is 5 pulses per s continuous operation.

## ACKNOWLEDGMENTS

This work was supported by DOE under Contract No. DE-AC03-87SF16731. We would like to thank Leo Brissette for actually building and/or assembling most of the hardware on RRAIDER and for helping to test it.

[1] T. A. Melhorn *et al.*, in *Proceedings of the Ninth International Conference on High-Power Particle Beams*, edited by G. Cooperstein, V. Granatstein, and D. Mosher (NTIS, Springfield, VA, 1992), p. 31.
[2] J. Katzenstein, S. Robertson, and N. Rostoker, in *Proceedings of the Fifth International Conference on High-Power Particle Beams*, edited by R. J. Briggs and A. J. Toepfer (LLNL, Livermore, 1983), p. 264.
[3] P. L. Dreike, J. B. Greenly, D. A. Hammer, and R. N. Sudan, Phys. Fluids **25**, 59 (1982).
[4] J. M. Finn and R. N. Sudan, Nucl. Fusion **22**, 1443 (1982).
[5] H. H. Fleischmann and T. Kammash, Nucl. Fusion **15**, 1143 (1975).
[6] N. Rostoker and A. Fisher, in *Proceedings of the Sixth International Conference on High-Power Particle Beams*, edited by C. Yamanaka (Kobe, Japan, 1986), p. 407.
[7] R. N. Sudan and E. Ott, Phys. Rev. Lett. **33**, 355 (1974).
[8] D. J. Rej, R. R. Bartsch, H. A. Davis, R. J. Faehl, J. B. Greenly, I. Hennis, T. W. Linton, and R. E. Meunchausen, in Ref. 1, p. 88.
[9] K. Yatsui, in *Proceedings of the Seventh International Conference on High-Power Particle Beams*, edited by W. Bauer and W. Schmidt (Karlsruhe, Germany, 1988), Vol. 1, p. 283.
[10] R. T. Hodgson, J. E. E. Baglin, R. Pal, J. M. Neri, and D. A. Hammer, Appl. Phys. Lett. **37**, 187 (1980).
[11] See, for example, G. E. Remnev and V. A. Shulov, in Ref. 1, p. 365.
[12] M. Gryzinski *et al.*, in Ref. 9, p. 319.
[13] G. A. Moses *et al.*, in Ref. 9, p. 113.
[14] J. B. Greenly, in Ref. 9, p. 137.
[15] S. Humphries, Jr., Nucl. Fusion **20**, 1549 (1980).
[16] T. Fessenden *et al.*, The Experimental Test Accelerator: Description and Results of Initial Experiments, Lawrence Livermore Laboratory Report No. UCID 18642, 1980.
[17] J. B. Greenly and Y. Nakagawa, Production of Fast Neutrals in Magnetically Insulated Diodes, Laboratory of Plasma Studies, Cornell University Report No. LPS 303, 1982.
[18] J. B. Greenly, M. Ueda, G. D. Rondeau, and D. A. Hammer, J. Appl. Phys. **93**, 1872 (1988).
[19] M. Ueda, Ph.D. dissertation, Cornell University, 1986; M. Ueda, J. B. Greenly, G. D. Rondeau, and D. A. Hammer, Rev. Sci. Instrum. **64**, 2737 (1993); Laser Particle Beams **12**, 585 (1994).

[20] W. A. Noonan and D. A. Hammer (unpublished); W. A. Noonan, Ph.D. dissertation, Cornell University, 1992.
[21] S. C. Glidden, W. A. Noonan, L. Brissette, and D. A. Hammer, *Proceedings of the Eight IEEE Pulsed Power Conference*, edited by R. White and K. Prestwich (IEEE, New York, 1991), p. 78.
[22] Society of Automative Engineers Manual on Design and Manufacture of Coned Disk Springs or Belleville Springs, New York, 1950.
[23] P. D. Pedrow, Ph.D. dissertation, Cornell University, 1985.
[24] S. C. Glidden and L. Brissette, *Proceedings of the Seventh IEEE Pulsed Power Conference*, edited by B. H. Bernstein and J. P. Shannon (IEEE, New York, 1989), p. 736.
[25] K. K. Jain, Characterization of the anode plasma by spectroscopy and Langmuir probe measurements on RRAIDER (unpublished).
[26] R. W. Stinnett *et al.*, Mater. Res. Soc. Symp. Proc. **316**, 521 (1994); T. J. Renk, R. W. Stinnett, K. P. Lamppa, D. C. McIntyre, R. G. Buchheit, and J. B. Greenly, Bull. Am. Phys. Soc. **39**, 1579 (1994).